

# On Irradiance Distributions for Weakly Turbulent FSO Links: Log-Normal vs. Gamma-Gamma

Carmen Álvarez Roa\*, Yunus Can Gültekin, Vincent van Vliet, Menno van den Hout, Chigo Okonkwo, and Alex Alvarado

Department of Electrical Engineering, Eindhoven University of Technology, Eindhoven, the Netherlands

\*[c.alvarez.roa@tue.nl](mailto:c.alvarez.roa@tue.nl)

**Abstract:** Weak turbulence is commonly modeled using the log-normal distribution. Our experimental results show that this distribution fails to capture irradiance fluctuations in this regime. The Gamma-Gamma model is shown to be more accurate. © 2026 The Author(s)

## 1. Introduction

Free-space optical (FSO) communications are considered a promising solution for establishing high-capacity point-to-point wireless links thanks to its large available unlicensed bandwidth. However, the performance of FSO systems is strongly impaired by atmospheric turbulence, which induces random irradiance fluctuations that can severely degrade the link reliability.

The strength of turbulence is commonly characterized by the Rytov variance ( $\sigma_R^2$ ). Depending on its value, different statistical models have been proposed to describe irradiance fluctuations [1, Fig. 7.4]. Under weak turbulence conditions ( $\sigma_R^2 < 1$ ), the log-normal (LN) distribution is traditionally employed [2]. The Gamma-Gamma (GG) distribution, in contrast, is commonly used for strong turbulence ( $\sigma_R^2 > 1$ ) [3]. In this work, we focus on the weak turbulence regime, where the scintillation index (SI)—a standard metric in FSO communications—provides a good estimate of the Rytov variance, i.e.,  $\sigma_R^2 \approx \text{SI}$  [1, Sec. 8]. Henceforth, we only consider SI in this paper.

The LN model is known to have limitations, particularly in capturing the tails of the probability density function (PDF) of the irradiance fluctuations. These tails are crucial for estimating the fade probability, i.e., the fraction of time the irradiance falls below a prescribed threshold [1, Sec. 9.9]. Nevertheless, the LN model continues to be widely used in the weak turbulence regime, as evidenced by several studies [4–8]. Moreover, previous studies conducted on the same experimental link considered in this paper have also adopted the LN model specifically to obtain the Rytov variance [9, 10]. By contrast, the GG distribution has been shown to provide good agreement with experimental measurements under strong turbulence [1, 3], but it is rarely applied in the weak turbulence regime. Previous experimental and numerical studies [1, 3, 8, 11, 12] have focused primarily on very weak turbulence regimes ( $\text{SI} \leq 0.13$ ), leaving the *intermediate weak turbulence regime* ( $0.13 < \text{SI} \leq 1$ ) largely unexplored. Consequently, the accuracy of both LN and GG models in describing weak turbulence within this range of SIs has not been thoroughly verified experimentally.

This paper presents an extensive experimental study of turbulence-induced irradiance fluctuations over a 4.6 km FSO link deployed above a dense urban area. This distance is considerably longer than those typically reported in previous studies (100 m–2.4 km) [7, 8, 11, 12]. In this paper, we use experimental data within the *intermediate weak turbulence regime* ( $0.13 < \text{SI} \leq 1$ ) to assess the validity of the LN and GG distributions. To the best of our knowledge, this work provides the first experimental evidence from a deployed FSO system indicating that the LN model does not accurately approximate the PDF of the irradiance in this range. Our results also show that the GG model consistently provides a more accurate fit.

## 2. Experimental Setup and Signal Analysis

A permanent FSO link has been established in Eindhoven, the Netherlands, connecting the Eindhoven University of Technology with the High Tech Campus. This link enables data transmission over a distance of 4.6 km. The optical link is deployed above a dense urban area, directly crossing over the city center, as shown in Fig. 1 [9]. The optical terminals from the development partner Aircision are equipped with automated beam tracking and alignment systems tip/tilt correction, continuously optimizing the free-space-to-fiber coupling. As a result, pointing errors are largely compensated and their contribution to the observed signal fluctuations is minimized, allowing the analysis to focus on turbulence-induced fading. A detailed description of the experimental setup can be found in [9, 10].

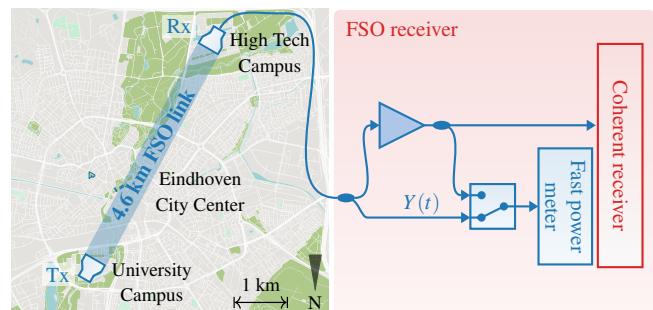


Figure 1: Experimental setup for an FSO link connecting Eindhoven University of Technology and the High Tech Campus over 4.6 km.

As shown in Fig. 1, the received optical power was continuously monitored with a high-speed power meter operating at 10 kSa/s. Using this setup, a 30-hour measurement campaign was carried out on 14–15 October 2024. To characterize the temporal fluctuations of the channel, the recorded data was analyzed in consecutive, nonoverlapping, one-minute windows. Let  $Y_k[n]$  be the  $n$ -th sample of the received optical power  $Y(t)$  (see Fig. 1) within the  $k$ -th one-minute window. The SI for the  $k$ th window is computed as

$$\text{SI}_k = \frac{\mathbb{E}\{Y_k[n]^2\} - \mathbb{E}\{Y_k[n]\}^2}{\mathbb{E}\{Y_k[n]\}^2}, \quad (1)$$

where  $\mathbb{E}\{\cdot\}$  indicates the expectation taken over the samples collected within the  $k$ -th window.

Following the approach of [11, Sec. V], we sort the values of  $\text{SI}_k$  to group one-minute windows with similar levels of turbulence. This procedure enables the estimation of representative PDFs under different turbulence conditions. To compensate for slow variations in the received optical power (e.g., caused by atmospheric attenuation), the signal within each one-minute window is normalized with respect to its mean. We therefore define the normalized samples of the received optical power  $\bar{Y}_k[n]$  and their mean  $\bar{\mu}_k$  as

$$\bar{Y}_k[n] \triangleq \frac{Y_k[n]}{\mathbb{E}\{Y_k[n]\}}, \quad \bar{\mu}_k \triangleq \mathbb{E}\{10\log(\bar{Y}_k[n])\}. \quad (2)$$

Fig. 2 presents the relationship between the sorted values of  $\text{SI}_k$  from (1) and their mean normalized power  $\bar{\mu}_k$  from (2). Fig. 2 (left) shows the evolution of the sorted data. A clear opposite trend is observed: higher SI values are associated with lower mean normalized power levels. The use of normalized power in (2) effectively removes the influence of long-term drifts or absolute power variations, resulting in a clearer and more physically meaningful correlation, which is not readily apparent in [9, Fig. 2]. Fig. 2 (right) presents the corresponding scatter plot (blue circles). Fig. 2 (right) shows a clear correlation between  $\text{SI}_k$  and  $\bar{\mu}_k$ . As shown in Fig. 2, the dataset corresponding to the 30-hour measurement period considered in this work spans both weak and strong turbulence regimes. In the following section, we focus exclusively on the weak turbulence regime ( $\text{SI} < 1$ ).

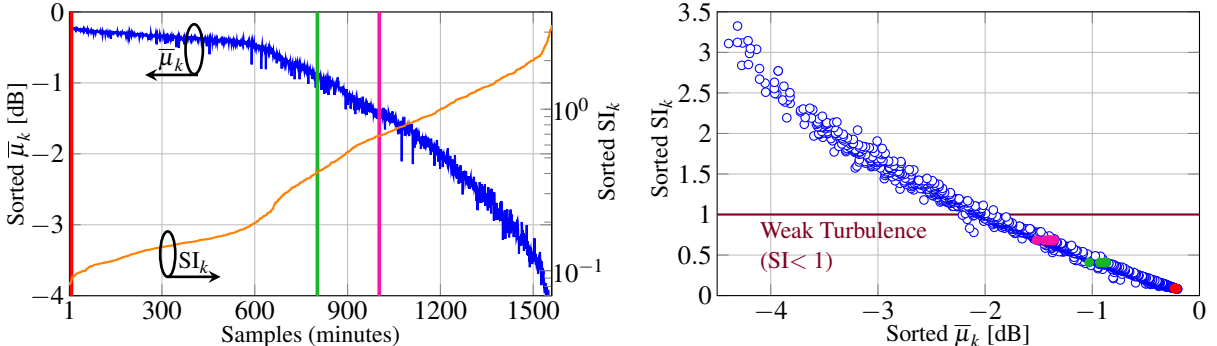


Figure 2: Sorted  $\text{SI}_k$  and  $\bar{\mu}_k$  (left), computed over one-minute windows and  $\text{SI}_k$ - $\bar{\mu}_k$  scatter plot (right).

### 3. Numerical Results

The LN and GG distributions are parametric distributions. We estimate these parameters ( $\sigma^2$  for LN and  $(\alpha, \beta)$  for GG) using maximum likelihood estimation [12, Sec. IV-C]. The sorted data is grouped into windows with similar SIs, following the method proposed in [11]. In our case, five consecutive one-minute windows are combined to form each grouped dataset. This five-minute grouping provides enough samples to accurately estimate the tails of the PDFs while keeping the parameters of the PDFs approximately constant during each dataset.

To illustrate representative turbulence conditions, three datasets were selected, corresponding to  $\text{SI} = 0.101$ ,  $\text{SI} = 0.486$ , and  $\text{SI} = 0.817$ . These datasets are indicated in Fig. 2 (left) by the vertical red, green, and pink lines, resp., and are highlighted in Fig. 2 (right) as colored circles using the same color scheme. Fig. 3 shows the corresponding PDFs obtained from these datasets. In each plot, the circles represent the normalized empirical PDF, while the dashed black and red curves correspond to the LN and GG distributions, resp.. The three subplots correspond to  $\text{SI} = 0.101$  (left),  $\text{SI} = 0.486$  (middle), and  $\text{SI} = 0.817$  (right). The horizontal axis represents the normalized received optical power within each five-minute data window. A logarithmic scale is used on the vertical axis to better visualize the tails of the PDFs, while the inset with linear scaling provides a clearer view of the peak of the PDFs.

The results for  $\text{SI} = 0.101$  (Fig. 3, left) provide an experimental validation of the conclusions reported in [1, 3] for  $\text{SI} \approx 0.1$ , which relied exclusively on simulation results. Consistent with these works, our measurements show that both the LN and GG models underestimate the left tail of the PDF. Fig. 3 (left) also shows that the GG model provides a noticeably better fit to the right tail of the PDF. Fig. 3 (middle) and Fig. 3 (right) present the results for  $\text{SI} = 0.486$  and  $\text{SI} = 0.817$ , respectively. These results show that the LN distribution underestimates both the

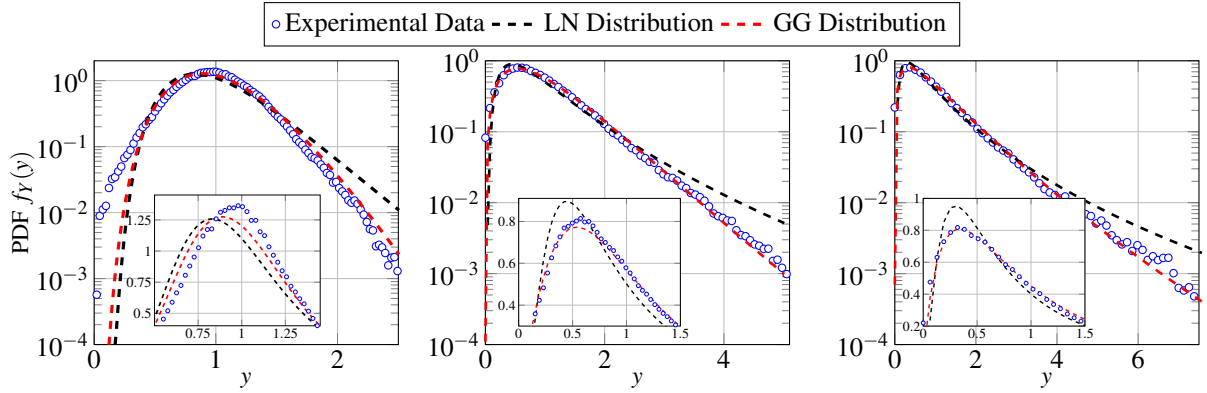


Figure 3: PDF of the normalized received optical power  $f_Y(y)$  under weak turbulence for experimental data. Results for the LN and GG distributions are also shown. Columns correspond to  $SI = 0.101$  (left),  $SI = 0.486$  (middle), and  $SI = 0.817$  (right).

peak and the right tail of the empirical PDFs, whereas the GG distribution closely matches the experimental data. Overall, across all three turbulence conditions, the GG distribution provides a significantly better fit to the empirical data than the LN model, particularly for the tails of the PDFs.

#### 4. Conclusions

We investigated the validity of the LN distribution for modeling weak atmospheric turbulence using measurements from a 4.6 km experimental FSO link crossing directly over the city center of Eindhoven. In contrast to previous studies, our dataset spans a much wider range of SI, extending into the *intermediate weak turbulence regime* ( $0.13 < SI \leq 1$ ) that has remained largely unexplored. Our analysis showed that, within this regime, the empirical PDFs exhibit clear deviations from the LN model. Specifically, the LN distribution overestimates the peak of the PDF and underestimates the distribution tails, which could lead to inaccurate predictions of deep fades, and, consequently, of outage probability. While similar trends have been observed for other SI ranges in numerical simulations, no prior experimental or numerical evidence exists for the SI range considered here. Our results provide direct experimental evidence that the LN model is inadequate for accurately describing weak turbulence conditions, where it is traditionally assumed to work well. Moreover, our results show that the GG model, often used only for strong turbulence, provides a more accurate fit across weak turbulence conditions, outperforming the LN model throughout the SI range considered.

**Acknowledgements:** This publication is part of the project BIT-FREE with file number 20348 of the research programme Open Technology Programme and of the project AI-SUSAT with grant ID OAARE97526 of the research programme AiNed XS Europe, which are (partly) financed by the Dutch Research Council (NWO). This research has received funding from the Project Optical Wireless Superhighways: Free photons (FREE) under Grant P19-13, the PhotonDelta National Growth Fund Programme on Photonics, and the European Innovation Council Transition project CombTools under Grant G.A. 101136978. The authors thank Aircision B.V., particularly Nourdin Kaai, Roland Blok, and Andreas Kotilis, for their support in setting up the High Tech Campus location of the Reid Photonloop FSO testbed. The authors also thank Prof. Eduard Tangdionga for his key contributions to the setup of the testbed.

#### References

1. L. C. Andrews and R. L. Phillips, "Laser Beam Propagation through Random Media," *SPIE*, 2005.
2. R. L. Phillips and L. C. Andrews, "Measured Statistics of Laser-light Scattering in Atmospheric Turbulence," *J. Opt. Soc. Am.*, vol. 71, no. 12, pp. 1440 – 1445, Dec. 1981.
3. A. Al-Habash, L. C. Andrews, R. L. Phillips, "Mathematical Model for the Irradiance Probability Density Function of a Laser Beam Propagating through Turbulent Media," *Opt. Eng.*, vol. 40, no. 8, pp. 1554 – 1562, Jan. 2001.
4. A. A. Farid and S. Hranilovic, "Outage Capacity Optimization for Free-Space Optical Links With Pointing Errors," in *JLT*, vol. 25, no. 7, pp. 1702 – 1710, July 2007.
5. G. Yang *et al.*, "Channel Modeling and Performance Analysis of Modulating Retroreflector FSO Systems Under Weak Turbulence Conditions," in *IEEE Photonics J.*, vol. 9, no. 2, pp. 1 – 10, April 2017.
6. M. T. Dabiri and S. M. S. Sadough, "Performance Analysis of All-Optical Amplify and Forward Relaying Over Log-normal FSO Channels," *JOCN*, vol. 10, no. 2, pp. 79 – 89, Feb. 2018.
7. Z. Nazari, A. Gholami, Z. Vali, M. Sedghi and Z. Ghassemlooy, "Experimental Investigation of Scintillation Effect on FSO Channel," *24th ICEE*, Shiraz, Iran, May 2016
8. M. A. Esmail, "Experimental Performance Evaluation of Weak Turbulence Channel Models for FSO Links," *Opt. Commun.*, vol. 486, no. 7, May 2021.
9. V. van Vliet, M. van den Hout, K. Gümüş, E. Tangdionga and C. Okonkwo, "5.7 Tb/s Transmission Over a 4.6 km Field-Deployed Free-Space Optical Link in Urban Environment," *OFC*, San Francisco, CA, USA, 2025.
10. V. van Vliet, M. van den Hout, K. Gümüş, E. Tangdionga and C. Okonkwo, "Experimental Investigation of Availability in a 4.6 km Terrestrial Urban Coherent Free-Space Optical Communications Link," *ECOC*, Copenhagen, Denmark, 2025.
11. J. H. Churnside and R. G. Frehlich, "Experimental Evaluation of Log-normally Modulated Rician and IK Models of Optical Scintillation in the Atmosphere," *J. Opt. Soc. Am. A*, vol. 6, no. 11, pp. 1760 – 1766, Nov. 1989.
12. A. Mostafa and S. Hranilovic, "Channel Measurement and Markov Modeling of an Urban Free-Space Optical Link," *JOCN*, vol. 4, no. 10, pp. 836 – 846, Oct. 2012.